

# The “soft ridge” – is it initial-state geometry or modified jets?

Thomas A. TRAINOR

*CENPA 354290, University of Washington, Seattle, WA 98195 USA*

An  $\eta$ -elongated same-side 2D peak (“soft ridge”) in minimum-bias angular correlations from heavy ion collisions has been attributed both to jet formation and to initial-state geometry structure coupled to radial flow. We consider evidence for both interpretations.

## §1. Introduction

A same-side (SS) 2D peak dominates minimum-bias angular correlations (no trigger-associated  $p_t$  cuts) for all A-A centralities at higher RHIC energies. In 200 GeV  $p$ - $p$  collisions the SS peak properties are consistent with minijets. The peak is elongated on  $\phi$ .<sup>1)</sup> In more-central Au-Au collisions the SS peak becomes elongated on  $\eta$ <sup>6)</sup> and is then described by some as a “soft ridge.” Recent initiatives reinterpret the “soft ridge” in terms of flows.<sup>2)-4)</sup> A recipe for assigning the SS 2D peak to (higher harmonic) flows has emerged: (a) Project (all or part of) the  $\eta$  acceptance onto azimuth  $\phi$ ; (b) fit the 1D projection on  $\phi$  with a Fourier series; (c) interpret each series term as a harmonic flow; (d) attribute the flows to conjectured A-A initial-state (IS) geometry. To better establish the true mechanism for the SS 2D peak we compare recent flow conjectures and a minijet interpretation within a 2D context.

## §2. Angular correlations from minimum-bias jets (minijets)

Substantial experimental and theoretical evidence supports the conclusion that SS 2D and away-side (AS) 1D peaks are manifestations of minimum-bias jets (minijets).<sup>1),5)-7)</sup> The monolithic minimum-bias SS 2D peak is well described by a 2D Gaussian with no additional ridge structure. The AS 1D peak is consistent with parton momentum conservation (dijets). AS correlation structure is uniform on  $\eta$ .

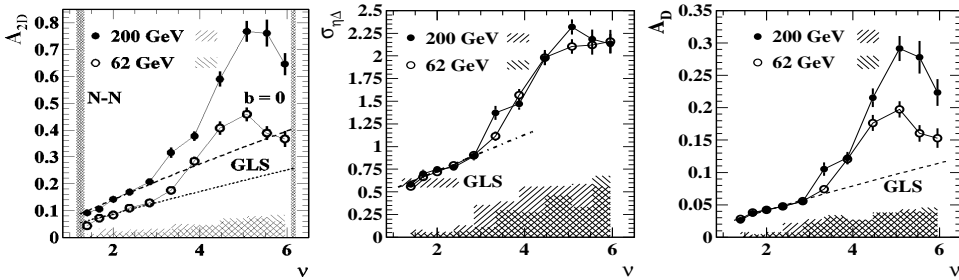


Fig. 1. First: SS 2D peak amplitude, Second: SS peak  $\eta$  width, Third: AS 1D peak amplitude.

Figure 1 shows Au-Au centrality trends for SS 2D and AS 1D peak parameters.<sup>6)</sup> The trends are consistent with minijets from Glauber linear superposition (GLS) of

N-N collisions up to a sharp transition at  $\nu \equiv 2N_{bin}/N_{part} \approx 3$ . Above that point deviations from GLS are consistent with modified parton fragmentation to jets.<sup>7),8)</sup>

### §3. SS 2D peak Fourier decomposition and “higher harmonics”

If the SS 2D peak is projected onto 1D azimuth the resulting 1D Gaussian has a Fourier series representation, the terms representing cylindrical multipoles. The jet-related quadrupole amplitude is  $2A_Q\{SS\} = 2\rho_0(b)v_2^2\{SS\} = F_2(\sigma_{\phi_\Delta})A_{1D}$ , where  $A_{1D}$  is the projected SS 1D peak amplitude,  $F_2(\sigma_{\phi_\Delta})$  is a Fourier coefficient and  $\rho_0(b)$  is the single-particle angular density. Figure 2 (first panel) shows Fourier coefficients for a unit-amplitude Gaussian with r.m.s. width  $\sigma_{\phi_\Delta} = 0.65$  (SS 1D peak width for more-central 200 GeV Au-Au collisions). The coefficients are given by  $F_m(\sigma_{\phi_\Delta}) = \sqrt{2/\pi} \sigma_{\phi_\Delta} \exp(-m^2\sigma_{\phi_\Delta}^2/2)$ . Thus, “higher harmonics” from the SS 2D peak can be predicted accurately from measured minijet systematics as in Fig. 1.

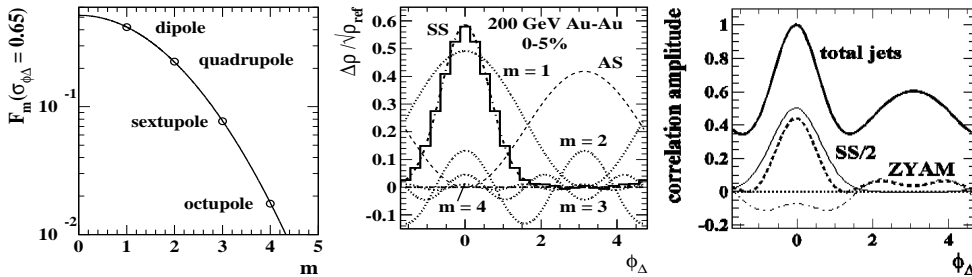


Fig. 2. First: Fourier coefficients, Second: SS peak Fourier components, Third: ZYAM subtraction.

Figure 2 (second panel) shows the measured SS 2D peak from 0-5% central Au-Au collisions projected onto azimuth (bold histogram).<sup>6)</sup> The fitted AS dipole (dashed curve) has been subtracted from the data histogram. RMS residuals from the 2D model fit are  $\approx 0.5\%$  of the SS peak amplitude, consistent with statistics. The multipole components of the SS 1D peak (dotted curves) are calculated from  $F_m$  and the SS peak parameters. For 0-5% central collisions the nonjet quadrupole  $A_Q\{2D\} \approx 0$ .<sup>9)</sup> The  $A_X\{SS\}$  ( $X = Q, S, O$ ) represent structures with large curvatures on  $\eta_\Delta$ , whereas  $A_Q\{2D\}$  represents a structure uniform on  $\eta_\Delta$  within the STAR TPC acceptance. The  $\eta_\Delta$  dependence permits accurate distinction between jet-related multipoles  $A_X\{SS\}$  (“nonflows”) and the nonjet quadrupole  $A_Q\{2D\}$ .

The *total* quadrupole from projected angular correlations is  $A_Q\{2\} = A_Q\{SS\} + A_Q\{2D\}$ . A similar expression holds for higher moments  $Q \rightarrow S, O$  (sextupole and octupole). The corresponding  $v_m$  derived from SS 2D peak parameters in Fig. 1 for 0-5% 200 GeV Au-Au are  $v_2\{2\} = 0.026$ ,  $v_3\{2\} = 0.015$  and  $v_4\{2\} = 0.007$ . By the same procedure “triangular flow” and higher multipoles can be derived from measured SS 2D peak systematics with various  $\eta$  exclusion cuts supposed to reduce or eliminate “nonflow.”<sup>10)</sup> “Higher harmonic flow” results from the LHC can be (and have been) anticipated by RHIC minijet and nonjet quadrupole measurements.<sup>10)</sup>

Figure 2 (third panel) illustrates ZYAM subtraction to infer jet structure from “triggered” dihadron correlations. The data (plotted relative to a zero offset deter-

mined by 2D model fits) are described by the bold solid curve. ZYAM subtraction with conventional  $v_2$  estimate from published data leads to the dashed curve: greatly reduced peak amplitudes and AS double peak. The dash-dotted curve is the sextupole from the SS jet peak plus the difference between SS and AS dipoles, explaining the AS double-peak structure. The jet inference is distorted and misleading.<sup>11)</sup>

#### §4. Comparing jet, nonjet quadrupole and IS geometry trends

Accurate distinction between jets and nonjet structures attributed to conjectured flows depends on careful differential comparisons among  $p_t$ ,  $\eta$  and centrality dependence of angular correlations. For example, the nonjet quadrupole  $A_Q\{2D\}$  inferred from 2D model fits to angular correlations is accurately distinguished from jet structure on the basis of the strong  $\eta$  dependence of the SS 2D peak.

Figure 3 (first panel) shows  $A_Q\{2D\}(b)$  data (solid curves) inferred from 2D model fits.<sup>9)</sup> The dashed curve is the same trend extrapolated to 17 GeV. The open square points and solid triangles represent  $A_Q\{EP\} \approx A_Q\{2\}$  transformed from published  $v_2\{EP\} \approx v_2\{2\}$  data.<sup>12),13)</sup> The  $A_Q\{2D\}$  data exhibit universal centrality and energy trends for a phenomenon independent of SS and AS jet structure.

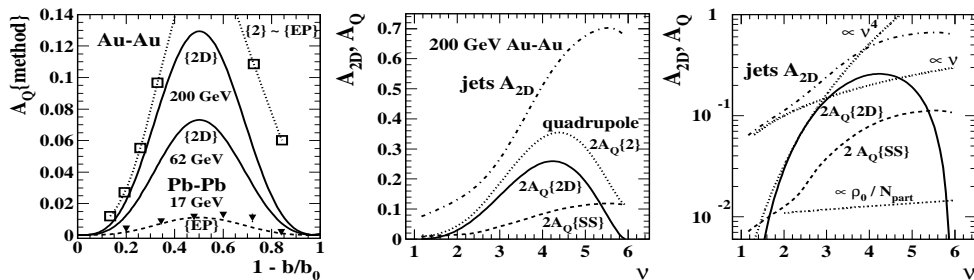


Fig. 3. First: Azimuth quadrupole, Second: Jet and nonjet trends, Third: Centrality comparisons.

Figure 3 (second panel) shows a direct comparison among jet and nonjet structures. The relation between  $v_2$  methods is given by  $A_Q\{2\} = A_Q\{SS\} + A_Q\{2D\}$ : jet-related plus nonjet quadrupoles sum to a total quadrupole amplitude measured by  $v_2\{2\} \approx v_2\{EP\}$ . “Nonflow” component  $2A_Q\{SS\} = F_2(\sigma_{\phi_\Delta})G(\sigma_{\eta_\Delta})A_{2D}(b)$  is the quadrupole component of the SS 2D peak projected onto azimuth.<sup>10)</sup> The  $v_2\{2\}$  inferred from that relation accurately describes published  $v_2$  data.<sup>10),14)</sup> The distinction between jet and nonjet structure is based on curvatures on  $\eta_\Delta$ .

Figure 3 (third panel) compares centrality trends for several correlation mechanisms. The nonjet quadrupole  $A_Q\{2D\}$  (bold solid curve) varies as  $N_{bin}\epsilon_{opt}^2 \propto v^4\epsilon_{opt}^2$ ,<sup>9)</sup> a very strong rate of increase for more-peripheral collisions. The SS 2D peak amplitude varies as  $N_{bin}/n_{ch} \approx v = 2N_{bin}/N_{part}$  (upper dotted curve) for Glauber linear superposition but increases more rapidly in Au-Au collisions above a sharp transition at  $v \approx 3$  (dash-dotted curve).<sup>6)</sup> The corresponding jet-related quadrupole  $A_Q\{SS\}$  (dashed curve) includes the effect of projecting the SS 2D peak onto 1D azimuth.<sup>10)</sup> All jet-related higher multipoles (“higher harmonic flows”) share the same centrality trend. The statistically compatible IS geometry measure

$\rho_0 \epsilon_{m,MC}^2$  (lower dotted curve) varies as  $\rho_0/N_{part} \approx \text{constant}$  for  $m$  odd.<sup>10)</sup> If those three elements are actually related to a common IS geometry through hydrodynamic flows why are the centrality trends so dramatically different?

### §5. Jets vs flows in a larger context

The correlation structures attributed separately to minijets and the nonjet quadrupole in 2D analysis can be compared in other contexts, including particle yields and  $p_t$  spectrum structure. Quadrupole  $p_t$  spectra can be inferred from  $v_2(p_t, b)$  data for unidentified and identified hadrons.<sup>15)</sup> The quadrupole component emerges from a boosted source with fixed boost independent of A-A centrality, and the quadrupole appears to be carried by a small fraction of the total hadron yield.<sup>16)</sup> Single-particle yields inferred from minijets plus a pQCD jet cross section agree with inferred spectrum hard-component yields.<sup>5),8)</sup> Spectrum hard-component systematics in turn agree with pQCD calculated parton fragment distribution.<sup>7)</sup> Glasma flux tubes as a mechanism for the SS 2D peak disagree with the  $p_t$  structure of correlations.<sup>18)</sup>

### §6. Summary

Minimum-bias 2D angular correlations include a monolithic same-side 2D peak, an away-side 1D peak described by a single dipole shape and a nonjet azimuth quadrupole represented by  $v_2\{2D\}$ . The SS 2D peak and AS 1D peak are quantitatively related to minimum-bias pQCD jets. Conventional  $v_m$  analysis ignores the  $\eta$  structure of the SS 2D peak. Consequently, Fourier components of the SS peak bias all  $v_m\{2\}$  data as “nonflows.” Recently announced “higher harmonic flows” are Fourier components of the SS peak. ZYAM subtraction of the jet-related quadrupole and higher harmonics is equivalent to subtracting jets from jets. In effect, parton fragmentation scenarios in nuclear collisions have been abandoned without regard to likely jet modifications (e.g.,  $\eta$  broadening) in the A-A collision environment.

### References

- 1) R. J. Porter and T. A. Trainor (STAR Collaboration), PoS **CFRNC2006**, 004 (2006).
- 2) B. Alver and G. Roland, Phys. Rev. C **81**, 054905 (2010).
- 3) S. Gavin, L. McLerran and G. Moschelli, Phys. Rev. C **79**, 051902 (2009).
- 4) P. Sorensen, J. Phys. G **37**, 094011 (2010).
- 5) T. A. Trainor and D. T. Kettler, Phys. Rev. C **83**, 034903 (2011).
- 6) G. Agakishiev *et al.* (STAR Collaboration), arXiv:1109.4380.
- 7) T. A. Trainor, Phys. Rev. C **80**, 044901 (2009).
- 8) T. A. Trainor, Int. J. Mod. Phys. E **17**, 1499 (2008).
- 9) D. T. Kettler (STAR collaboration), Eur. Phys. J. C **62**, 175 (2009).
- 10) T. A. Trainor, arXiv:1109.2540.
- 11) T. A. Trainor, Phys. Rev. C **81**, 014905 (2010).
- 12) A. M. Poskanzer *et al.* (NA49 Collaboration), Nucl. Phys. A **661**, 341 (1999).
- 13) J. Adams *et al.* (STAR Collaboration), Phys. Rev. C **72**, 014904 (2005).
- 14) T. A. Trainor, Mod. Phys. Lett. A **23**, 569 (2008).
- 15) T. A. Trainor, Phys. Rev. C **78**, 064908 (2008).
- 16) D. Kettler (STAR Collaboration), J. Phys. Conf. Ser. **270**, 012058 (2011).
- 17) T. A. Trainor and D. T. Kettler, Phys. Rev. C **83**, 034903 (2011).
- 18) T. A. Trainor and R. L. Ray, Phys. Rev. C **84**, 034906 (2011).